RELATIONS BETWEEN NOTCH STRESS AND CRACK STRESS INTENSITY APPLIED TO WELDED JOINTS

DIETER RADAJ and SHICHENG ZHANG
Daimler-Benz AG, Stuttgart, Germany

ABSTRACT

The limit value formulae for the stress intensity factors K_I, K_{II} and K_{III} proceeding from maximum notch stresses are reexamined with emphasis on the "abnormal" situation in plane shear loading. Fictitious notch rounding according to Neuber's microstructural support hypothesis is revised on that basis, extended to mixed mode loading and applied to cruciform welded joints subjected to fatigue loading.

KEYWORDS

Stress intensity factor, notch stress assessment, fatigue strength, welded joint

INTRODUCTION

Design and analysis of engineering structures are being performed more and more on the basis of local concepts which supplement or even substitute the former global concepts. Nominal stress assessment is considered to be a first step only. Structural stress assessment based on finite element analysis is a well established engineering procedure. Notch stress assessment in respect of crack initiation is additionally performed as far as possible ending up with a fracture mechanics analysis in respect of crack propagation and final fracture.

In recent years, major progress has been achieved in predicting the high cycle fatigue strength of welded joints and structures based on the notch stress approach. Following a proposal by Radaj [1, 2], the notches at the toe, root or end of seam welds, at the edge of weld spots and at other types of weld are fictitiously rounded according to Neuber's microstructural support hypothesis [3, 4]:

$$\rho_f = \rho + s\rho^* \qquad (1)$$

The fictitious notch radius ρ_f results from the actual notch radius ρ, the microstructural support length ρ^* (a material constant) and the factor s which depends on loading type and strength hypothesis.

It is sufficient for assessments of the least possible strength to neglect the actual small notch radius completely ($\rho = 0$), so that $\rho_f = s\rho^*$. Introducing $s = 2.5$ (tension load, plane stress, distortion strain energy hypothesis) and $\rho^* = 0.4$ mm (structural steel in cast condition), the result is $\rho_f = 1$ mm. The notches in welded joints in steel are fictitiously rounded with that radius, Fig. 1. A notch stress analysis is performed on the fictitiously rounded model. The maximum notch stress is compared with the fatigue strength values of unnotched specimens.

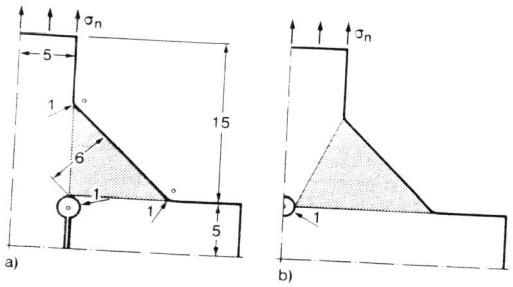

Fig. 1. Tension loaded cruciform welded joints; transverse stiffener joint with fillet welds (a) and cruciform joint with double-bevel butt welds (b), cross sectional models of symmetry quarter drawn with $\rho_f = 1$

This procedure produces reliable results, as has been shown by Radaj [2], Petershagen [5], Seeger and Olivier (see details in Ref. [2]). Despite the success in application, the following questions, more theoretical than practical in content, remain open:

- The introduced factor s = 2.5 is not valid in plane or antiplane shear loading.
- The relations for mixed mode slit tip loading are unknown.
- Tension loading in the direction of the slit causes no stress singularity or stress concentration but a fictitious hole does.
- Fictitious rounding of short slits resulting in a complete circle does not comply with the assumptions introduced when developing the procedure.
- Fictitious slit tip rounding in thin plate welded joints may diminish the load bearing cross section resulting in a stress rise which has nothing to do with the notch stress concentration.

In this paper answers are given to the above questions.

LIMIT VALUE FORMULAE FOR STRESS INTENSITY FACTORS

The limit value for the stress intensity factors proceeding from the stresses of the elliptical hole are well known:

$$K_I = \lim_{\rho \to 0} \frac{1}{2} \sigma_{max} \sqrt{\pi \rho} \qquad (K_{II} = K_{III} = 0) \tag{2}$$

$$K_{II} = \lim_{\rho \to 0} \sigma_{max} \sqrt{\pi \rho} \qquad (K_I = K_{III} = 0) \tag{3}$$

$$K_{III} = \lim_{\rho \to 0} \tau^*_{max} \sqrt{\pi \rho} \qquad (K_{II} = K_I = 0) \tag{4}$$

The authors [6] have added the following equation which correlates the maximum shear stress with the shear stress intensity factor:

$$K_{II} = \lim_{\rho \to 0} \frac{3\sqrt{3}}{2} \tau_{max} \sqrt{\pi \rho} \tag{5}$$

Whereas formula (5) is physically significant, formula (3) is of a more formal character (σ_{max} occurs beside the apex of the notch and is not a shear stress).

The authors [6] have generalized the formulae (2 - 4) by considering the ligament stresses as strength determinants thus removing the restrictions in (2 - 4) and allowing the use of a strength hypothesis in cases of superimposed (i. e. "mixed") slit loading. The antisymmetric part of the notch stresses must be evaluated to get σ_{max} (hereinafter designated as σ'_{max}) if (3) is used instead of (5).

The authors [6] have additionally modified equation (3) which was derived for elliptical notches for application on notches with a circular shape correlating the local maximum stress σ'_{max} with the local radius of curvature ρ':

$$K'_{II} = \lim_{\rho \to 0} \frac{1}{1.682} \sigma'_{max} \sqrt{\pi \rho} \tag{6}$$

CONVERGENCE OF LIMIT VALUE FORMULAE

The convergence behaviour of the limit value formulae should be known in cases of practical application. On the other hand, in practical application the elliptical notch is often replaced by a U-shaped or keyhole notch, which provides an exact circle at the root of the notch independent of gap width. Such notches are introduced in connection with fictitious notch rounding according to Neuber, simulating the microstructural support effect.

The investigation covered the plane shear (τ_n) loaded rectangular plate (width 2w, length 2l) with central crack or slit (length 2a) in comparison to an elliptical hole (length 2a, width 2b, notch radius $\rho = b^2/a$), a U-shaped hole (length 2a, width 2b = 2ρ) and a keyhole (length 2a, width zero), Fig. 2.

At first, the stress intensity factor $k_{II} = K_{II}/\tau_n\sqrt{\pi a}$ was calculated using the boundary element method, evaluating K_{II} from crack edge displacements and ligament stresses near the crack tip. The result was $k_{II0} = 1.360$.

Then the notch stresses at the comparable elliptical hole, U-hole and keyhole with very small notch radii ($\rho/a = 0.1, 0.01, 0.001, 0.0001$) were determined using the same method, evaluating $k_{II\sigma} = K_{II}/\tau_n \sqrt{\pi a}$ from (3) or $k'_{II\sigma} = K'_{II}/\tau_n \sqrt{\pi a}$ from (6) and $k_{II\tau} = K_{II}/\tau_n \sqrt{\pi a}$ from (5) and plotting them against ρ/a in order to find a suitable extrapolation scheme onto $\rho/a = 0$. The result is shown in Fig. 3.

The following conclusions are drawn:

- The relations (3) and (5) converge to the same correct K_{II} value in the case of the elliptical notch (but not so (6), as expected).
- Very small ρ/a values ($\rho/a = 0.001$) are necessary to get acceptable convergence.
- A suitable general extrapolation scheme to $\rho/a = 0$ has not been derived, but nonlinear extrapolation of larger ρ/a to $\rho/a = 0.0001$ seems to be acceptable.

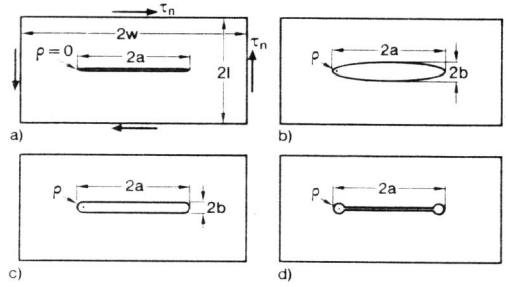

Fig. 2. Plane shear loaded rectangular plate with central crack or slit (a), elliptical hole (b), U-shaped hole (c) and keyhole (d)

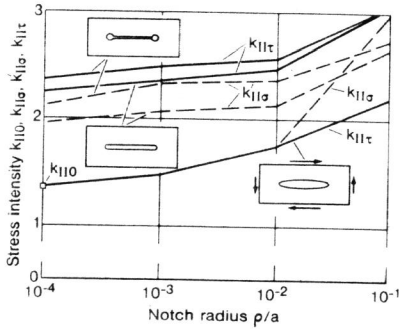

Fig. 3. Stress intensities (mode II) derived from crack (k_{II0}), elliptical hole, U-shaped hole and keyhole in plane-shear loaded rectangular plate, convergence behaviour of limit value formulae with ρ/a -> 0

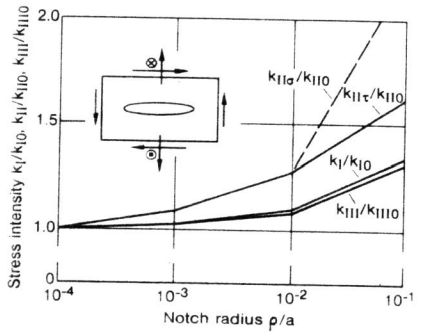

Fig. 4. Stress intensities (mode I, II and III) derived from elliptical hole in rectangular plate subjected to tension loading, plane shear loading and antiplane shear loading, convergence behaviour of limit value formulae with ρ/a -> 0

- There are only minor differences between $k_{II\sigma}$ and $k_{II\tau}$ in the case of the elliptical hole with the exception of large ρ/a (due to the effect on $k_{II\sigma}$ of the nearby horizontal plate edge).
- The relations (6) and (5) converge to roughly the same K_{II} value in the case of the U-notch and keyhole notch (but not so (3), as expected).
- The $k'_{II\sigma}$ values are slightly smaller than the $k_{II\tau}$ values.
- The keyhole notch gives slightly higher $k'_{II\sigma}$ and $k_{II\tau}$ values than the U-notch.
- The $k'_{II\sigma}$ and $k_{II\tau}$ values of U-notch and keyhole notch are larger than the $k_{II\sigma}$ and $k_{II\tau}$ values of the elliptical notch by the factor 1.44-1.74.

A comparison has been made of the convergence behaviour of k_I, k_{II} and k_{III} from mode I, mode II and mode III loading of the rectangular plate with elliptical hole, Fig. 4. The poor convergence of k_{II} in relation to k_I and k_{III} can be clearly seen.

COMPLICATION WITH THE LIMIT VALUE FORMULA FOR STRESS INTENSITY FACTOR K_I

A complication, hitherto not mentioned in the literature, may arise with the determination of K_I from σ_{max} in the apex $\varphi = 0$. Tension loading σ_0 in the direction of a crack introduces no stress singularity, whereas the same loading of an elliptical, U-shaped or keyhole notch causes high notch stresses near the apex points $\varphi = \pm \pi/2$ (concentration factor $\sigma^{**}_{max}/\sigma_0 \approx 2.0$) and a lower notch stress of

opposite sign, $\sigma^*_{max}/\sigma_0 \approx -1.0$, in the apex point $\varphi = 0$ (see Ref. [6]). Whereas the former is eliminated by evaluating the stresses in the ligament, the latter is not. This secondary stress σ^*_{max} may be comparable to or even larger than σ_{max} in the apex point from tension loading transverse to the crack. The secondary stress σ^*_{max} may therefore introduce a possibly large error into the determination of K_I from (2) (with or without the restriction $K_{II} = K_{III} = 0$).

The following procedure may be applied in more complex cases occuring in practice. The mean stress σ^*_m at the two slit edges outside the slit tips is set equal to σ_0 (after subtraction of the edge stress caused by global tension or compression transverse to the slit, i. e. the negative value of this tension or compression under the assumption of contact-free slit edges). The maximum stress σ^*_{max} is approximated by $\sigma^*_{max} \approx -\sigma_0$ (deviations occur with changing geometry and dimensions of the problem at hand). It is subtracted from σ_{max} before evaluating K_I.

The procedure must be applied in an iterative way if the (global) tension or compression transverse to the slit is not known in advance.

FICTITIOUS NOTCH ROUNDING IN PLANE SHEAR AND SUPERIMPOSED LOADING

Notch rounding according to Neuber for taking the microstructural support effect into account has so far only been applied in mode I and mode III loading of sharp notches and cracks propagating into the ligament, i. e. without a kink (with factor s = 2.0 - 3.0 for tension loading and s = 0.5 for antiplane shear loading).

The factor s in mode II loading is determined by equating the medium shear stress τ_m at the sharp crack tip averaged over length ρ^* of the ligament to the maximum shear stress τ_{max} of the fictitiously rounded crack tip according to Ref. [6]. This results in:

$$\rho_f = \frac{2}{27}\rho^* = 0.074\rho^* \tag{7}$$

When evaluating the stresses on the ligament, the factor s = 0.074 in mode II loading is (just as in mode III shear loading) independent of the strength hypothesis because pure shear loading is acting on the ligament.

When evaluating σ'_{max} which characterizes the antisymmetric part of the edge stresses as a substitute for τ_{max} the result according to Ref. [6] is:

$$\rho_f = \frac{1}{2}\rho^* \tag{8}$$

$$\rho'_f = \frac{(1.682)^2}{2}\rho^* = 1.415\rho^* \tag{9}$$

When evaluating the edge stresses of the elliptical notch, the factor s = 0.5 according to (8) is the same as in mode III shear loading. When evaluating the edge stresses of the circular notch, the factor s = 1.415 according to (9) is more in the range of mode I tension loading (s = 2.0 in plane stress with different strength hypotheses according to Ref. [3]). Both factors are independent of the strength hypothesis but the precondition is that the crack propagates into the ligament and does not kink.

Whereas different ρ_f values in plane and antiplane loading present no problem because a different software is used for calculating the notch stresses, the difference in s values for superimposed mode I and mode II loading necessitates a supplementary derivation step if only one simulation with one radius ρ_f is to be applied. This step modifies $\overline{\sigma}'_{max}$ or $\overline{\tau}_{max}$ (same square root dependency on ρ_f) to take the actual ρ_f into account.

Applying the distortion strain energy hypothesis to $\bar{\sigma}_{max}$ with s = 2.0, $\bar{\tau}_{max}$ with s = 0.074 and $\bar{\tau}^*_{max}$ with s = 0.5 to be superimposed on the ligament, the von Mises equivalent stress $\bar{\sigma}_{eq\ max}$ is:

$$\bar{\sigma}_{eq\ max} = \sqrt{\bar{\sigma}^2_{max\ 2.0} + 3\bar{\tau}^2_{max\ 0.074} + 3\bar{\tau}^{*2}_{max\ 0.5}} \tag{10}$$

When introducing $\bar{\sigma}'_{max\ 0.5} = 2.598\ \bar{\tau}_{max\ 0.5} = 2.598\sqrt{0.074/0.5}\ \bar{\tau}_{max\ 0.074} = \bar{\tau}_{max\ 0.074}$, the result is:

$$\bar{\sigma}_{eq\ max} = \sqrt{\bar{\sigma}^2_{max\ 2.0} + 3\bar{\sigma}'^2_{max\ 0.5} + 3\bar{\tau}^{*2}_{max\ 0.5}} \tag{11}$$

When using the fictitious radius with s = 2.0 from mode I in mode II and mode III as well, the result for the elliptical notch is:

$$\bar{\sigma}_{eq\ max} = \sqrt{\bar{\sigma}^2_{max\ 2.0} + 12\bar{\sigma}'^2_{max\ 2.0} + 12\bar{\tau}^{*2}_{max\ 2.0}} \tag{12}$$

With s = 1.415 according to (9) (instead of s = 0.5) for $\bar{\sigma}'_{max\ 1.415}$ in (11), the result is identical because $\bar{\tau}_{max\ 0.074}$ in (10) is the same. In case of a U-notch or keyhole notch, this shear stress must be diminished by a factor of about 1.6 (see Fig. 3), resulting in:

$$\bar{\sigma}_{eq\ max} = \sqrt{\bar{\sigma}^2_{max\ 2.0} + 4.7\bar{\sigma}'^2_{max\ 2.0} + 12\bar{\tau}^{*2}_{max\ 2.0}} \tag{13}$$

MAXIMUM STRESS EVALUATION AFTER FICTITIOUS NOTCH ROUNDING

Fictitiously rounding of the toe and root notches of welds and evaluating of the maximum stress of each notch without a more detailed analysis has been proposed in respect of welded joints and also performed with some success. Can this procedure be substantiated?

The procedure is, at least in principle, consistent with the maximum tangential stress hypothesis (according to Erdogan and Sih), which predicts crack initiation normal to the direction of this stress in case of superimposed mode I and mode II loading resulting in pure mode I loading of the propagating kinked crack. It is necessary for this tentative interpretation that σ_{max} is evaluated without the notch effect of equidirectional loading.

In case of cracks or slits with equidirectional load effect another interpretation consistent with practical situations is possible. The fictitiously rounded notch may directly simulate a crack or slit kinked in the direction normal to $\bar{\sigma}_{max}$ (e. g. due to a welding defect). The assumption must then be introduced that Neuber's hypothesis and formulae are valid also for cracks or slits with kinked ends which may be the case within acceptable accuracy limits.

An alternative procedure is to calculate K_I and K_{II} for the (unkinked) crack or slit tip, to convert the latter into notch stresses using Creager's equations for blunt cracks and to evaluate the maximum notch stress for superimposed mode I and mode II loading. A valuable secondary effect of this procedure is the fact that no cross sectional reduction by fictitious rounding occurs the correction of which may be problematic with the usual weld shape geometries.

When fictitiously rounding short cracks or slits so that a circular notch ($a = \rho_f$) is generated, the resulting maximum notch stress is overestimated.

Cracks or slits shorter than $a = 4\rho^*$ with σ_n, $a = 0.39\ \rho^*$ with τ_n and $a = 1.5\ \rho^*$ with τ^*_n have a lower σ_{max}, τ_{max} or τ^*_{max} than is shown by the stress concentration at the fictitious hole (see Ref. [6]). The short crack is higher in strength than the circular hole because the stress concentration of the hole is determined without microstructural support effect.

APPLICATION TO CRUCIFORM WELDED JOINTS

Some of the findings of the preceding chapters are now applied to the analysis of tension loaded cruciform joints, comprising the transverse stiffener joint with fillet welds and the cruciform joint with double-bevel butt welds, Fig. 1. The transverse stiffener joint has long slits (slit length 2a = 10 mm) in the direction of tension loading. The slit tips are mainly subjected to plane shear loading (mode II). The cruciform joint with double-bevel butt welds has short slits (slit length 2a = 2 mm) transverse to the direction of tension loading. The slit tips are mainly subjected to cross tension loading (mode I).

The models are investigated with sharp slit tips, with small fictitious slit tip radius ($\rho_f/a = 0.01$ and $\rho_f/a = 0.02$ respectively) and with large fictitious slit tip radius ($\rho_f/a = 0.2$ and $\rho_f/a = 1.0$ respectively). The large slit tip radius $\rho_f = 1$ mm corresponds to mild steel ($\rho_f = 2.5\ \rho^* = 1$ mm applied in [2] interpreted here as $\rho_f = 2.0\ \rho^* = 1$ mm in keeping with the preceding derivations). The edge stresses in the latter case are plotted together with loading and support forces in Fig. 5. The maximum (notch) stresses are indicated by fatigue notch factors K_f with indices t for weld toe and r for weld root.

The application-relevant parameter is the fatigue notch factor K_f which is identical with the ratio $\bar{\sigma}_{eq\ max}/\sigma_n$ if the relevant value of ρ^* is introduced ($\rho^* = 0.5$ mm for welded joints in steel). When applying Neuber's mean stress hypothesis to the singular stress increase at the slit tip directly, the result for the long slits of the transverse stiffener joint is (with $k_I = K_I/\sigma_n\sqrt{\pi a}$ and $k_{II} = K_{II}/\sigma_n\sqrt{\pi a}$):

$$K_f = \sqrt{k_I^2 + 31.64k_{II}^2}\sqrt{\frac{2a}{\rho^*}} \tag{14}$$

This avoids any reduction of load carrying cross sections which may occur with fictitious notch rounding.

When applying Neuber's mean stress hypothesis to the short transverse slits of the cruciform joint with double-bevel butt welds (with $k_{II} \approx 0$), the following formula is derived:

$$K_f = k_I\sqrt{\frac{2a}{\rho^*}} \tag{15}$$

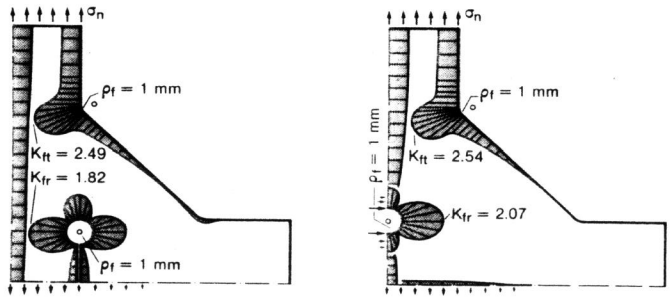

a) Transverse stiffener joint

b) Cruciform joint

Fig. 5. Notch stresses at transverse stiffener joint with fillet welds (a) and cruciform joint with double-bevel butt welds (b) subjected to tension loading, fatigue notch factors K_f for weld toe (index t) and weld root (index r), the latter uncorrected

Table 1: Stress intensity and fatigue notch factors of transverse stiffener joint with fillet welds

$\rho_f/a = 0$		$\rho_f/a = 0.01$			$\rho_f/a = 0.2$		
k_I	k_{II}	k_I	k_{II}	k'_{II}	k_I	k_{II}	k'_{II}
- 0.119	0.032	- 0.130	0.042	0.039	- 0.173	0.078	0.054
K_f from (14)		$\bar{\sigma}_{eq\ max}/\sigma_n$ from (13)			K_f from (13)		
0.965		3.243			0.927		

Table 2: Stress intensity and fatigue notch factors of cruciform joint with double-bevel butt welds

$\rho_f/a = 0$		$\rho_f/a = 0.02$		$\rho_f/a = 1.0$		
k_I	K_f	k_I	$\bar{\sigma}_{eq\ max}/\sigma_n$	k_I	k^*_I	K^*_f
0.658	1.316	0.654	9.252	1.035	0.732	1.464

The analysis results for the slit tip of the transverse stiffener joint (2a = 10 mm) are summarized in Table 1 (see Ref. [6] for details). The comparison of precise ($\rho_f/a = 0$) and approximated ($\rho_f/a \neq 0$) values shows that even with the large slit tip radius not too bad approximations of fatigue notch factor and stress intensity factors are determined. The conventional evaluation of the maximum boundary stress results in a too high fatigue notch factor (K_f = 1.82, see Fig. 5).

The analysis results for the slit tip of the cruciform joint with double-bevel butt weld (2a = 2 mm) are summarized in Table 2 (see Ref. [6] for details). The comparison of precise ($\rho_f/a = 0$) and approximated ($\rho_f/a \neq 0$) values shows rather poor correspondence. A better approximation is achieved according to $k^*_I = (1/2)(\bar{\sigma}_{max}/\sigma_n)/\sqrt{1 + a/\rho_f}$ which may be proposed as a short-crack corrected relation. The same corrective factor may be applied directly on σ_{max}/σ_n resulting in $K^*_f = (\bar{\sigma}_{max}/\sigma_n)/\sqrt{1 + a/\rho_f}$. The conventional evaluation of the maximum boundary stress results in a too high fatigue notch factor (K_f = 2.07, see Fig. 5).

It can be concluded that the risk of crack initiation at the weld root of the considered cruciform joints is markedly lower than stated in Fig. 5 as far as crack propagation in the direction of the slit can be assumed. The fatigue notch factors are reduced from 1.82 to 0.97 for the transverse stiffener joint with fillet welds and from 2.07 to 1.32 for the cruciform joint with double-bevel butt welds. On the other hand, crack initiation and propagation in the direction of the slit is an unrealistic assumption at least for the transverse stiffener joint. The original higher factor which is consistent with a crack in the direction of the maximum boundary stress is closer to reality. The reduction for the short slit in the cruciform joint is realistic because the crack will initially keep the direction of the slit.

REFERENCES

[1] Radaj, D.: Kerbwirkung von Schweißstößen hinsichtlich Ermüdung. Konstruktion 36 (1984) No. 8, pp. 285 - 292

[2] Radaj, D.: Design and analysis of fatigue resistant welded structures. Abington Publishing, Cambridge 1990

[3] Neuber, H.: Über die Berücksichtigung der Spannungskonzentration bei Festigkeitsberechnungen. Konstruktion 20 (1968) No. 7, pp. 245 - 251

[4] Neuber, H.: Kerbspannungslehre. Springer-Verlag, Berlin 1985

[5] Petershagen, H.: A comparison of different approaches to the fatigue strength assessment of welded components. IIW-Doc. XIII-1208-86, London 1986

[6] Radaj, D.; Zhang, S.: On the relations between notch stress and crack stress intensity in plane shear and mixed mode loading. IIW-Doc. XIII-1444-92, London 1992